Preprints of the 21st IFAC World Congress (Virtual)
Berlin, Germany, July 12-17, 2020

Sparsity Constrained Reconstruction for Electrical Impedance Tomography

Ganesh Teja Theertham, * **Santhosh Kumar Varanasi,** ** **Phanindra Jampana** *

* *Department of Chemical Engineering, Indian Institute of Technology Hyderabad, Kandi, Sangareddy, Telangana- 502285, India (e-mail: ch18mtech11007@iith.ac.in, pjampana@iith.ac.in).*
** *Department of Chemical and Materials Engineering, University of Alberta, Edmonton, T6G 1R1, Canada (e-mail:skvarana@ualberta.ca).*

Abstract: Electrical Impedance Tomography (EIT) can be used to study the hydrodynamic characteristics in multi-phase flows such as gas holdup in bubble columns, air-core in hydrocyclone, etc. In EIT, the main objective is to estimate the electrical properties (conductivity distribution) of an object in a region of interest based on the surface voltage measurements. The main challenge in such reconstruction (estimation of conductivity distribution) is the low spatial resolution. In this paper, a sparse optimization approach for image reconstruction in EIT is presented. The main idea presented in this article is based on considering the L_1 norm on the data term, which enhances the reconstruction of conductivity distributions with sharp changes near phase boundaries. Further, this method is also robust to outliers in the data. The accuracy of the proposed method is demonstrated with the help of two phantoms, and a comparison with the existing methods is also presented.

Keywords: Parameter estimation, Electrical Impedance Tomography, Sparse optimization, Interior point method.

1. INTRODUCTION

Tomography techniques are popular for visualizing the hydrodynamics of multi-phase flows in industrial processes. In Electrical Impedance Tomography, the electrical properties at a region of interest are computed from the surface measurements of electric potentials. These surface potentials are obtained by the application of small currents (e.g., ten milli-Amperes) to a pair of electrodes that are placed around the boundary. This procedure can be thought of as introducing a perturbation to a set of electrodes and procuring the data from the remaining successive pairs of electrodes. Although this technique was initiated for lung imaging (Borsic et al., 2010), it has gained importance in chemical processes for investigation of dispersion characteristics in multi-phase flows (Vadlakonda and Mangadoddy, 2018) and air-core characteristics in hydrocyclones (Varanasi et al., 2019). With multiple advantages such as being a non-invasive, low-cost, portable with immediate response characteristics (Bera, 2018), Electrical Resistance Tomography (which is the direct current analog of EIT) can be considered as a prime technique on par with its precedents such as Positron Emission Tomography, Computed Tomography which may cause adverse effects when used for longer periods.

The main challenge of reconstruction in EIT problem is that the continuous conductivity distribution needs to be recovered from a few voltage measurements at the boundary (Borsic et al., 2010) which makes the problem severely ill-posed. The classical back-projection algorithm (Santosa and Vogelius, 1990) and its variants such as modified sensitivity back projection (Kotre, 1994) are based on small perturbation approximations. Several regularization methods such as Tikhonov, Total Variation (TV) are used to alleviate the ill-posed nature directly. The main idea behind these methods is the inclusion of apriori information.

The current paper uses sparse constraints to drive the optimization of the regularized method to the desired solution. Sparsity refers to the number of non-zero components in a vector. Although the conductivity distribution may not be sparse (i.e., containing a large number of zero values) in chemical process applications, the gradient of conductivity is sparse with abrupt changes at the phase boundaries.

For example, in a hydrocyclone, there would be a sharp change in the conductivity at the boundary of the air-core. Similarly, sudden changes in conductivity would occur at the boundaries between the bubbles (gas phase) and the liquid phase in a bubble column.

The $L_1 - L_1$ method (Borsic and Adler, 2012) uses the 1-norm of the conductivity whereas the TV methods include the 2-norm on the gradient as regularizing terms. The L_1 method is known to provide sparse conductivity distributions, whereas the TV norm results in sparse conductivity gradients. However, these methods use convex relaxations, i.e., the 1-norm and the TV-norm respectively, instead of the true 0-norm, which is defined as the number of non-zero components of a vector.

The 0-norm has been incorporated directly into the regularization term in (Varanasi et al., 2019). Although this approach performs better than the previous methods, sharp conductivity profiles were not achieved accurately. This might be because considering L_2 norm on the data fit term makes the algorithm sensitive to outliers. To improve the reconstruction of images with sharp/abrupt changes and to make the algorithm more robust to outliers, a constraint of L_1 norm, is considered in the data fit in this paper. The 1-norm makes the optimization problem more challenging and a primal-dual interior point method (Borsic and Adler, 2012), combined with sparse optimization, is used for the solution.

The remainder of the paper is organized as follows. In Section 2, the problem statement is presented, and the mathematical framework to solve the reconstruction problem is detailed. Section 3 shows the application of the proposed method on two case studies in multi-phase flows. The results on normal, as well as data with outliers, are then compared with existing algorithms in Section 4. Section 5 provides the concluding remarks.

2. FORMULATION

2.1 Problem Statement

The governing equations of EIT are obtained using Maxwell's equations resulting a 2^{nd} order partial differential equation $\nabla.(\sigma(\omega)\nabla\phi(\omega)) = 0$, involving conductivity distribution (σ) and the electrical potential (ϕ) in the region of interest $(\omega \in \Omega)$.

The *forward problem* in EIT is to solve the Maxwell's equation to obtain the electric potential ϕ given the conductivity $\sigma(\omega)\ \forall\omega \in \Omega$. In practice, the solution to the *forward problem* is obtained using Finite Element Methods (FEM). For a given conductivity distribution (σ) let Γ_σ denote the function which maps the boundary surface voltage to boundary surface current. The *theoretical inverse* problem is to find σ given the map Γ_σ. Note that the knowledge of all possible boundary distributions of voltage and current pairs is required to formulate the map Γ_σ.

The *numerical reconstruction* problem is to compute the σ from a finite set of boundary surface voltage measurements. Let $F(\sigma)$ represent the boundary voltages predicted by solving the (PDE) e.g. using Finite Element Method (FEM), given conductivity (σ). Let $V_{\text{meas}} \in \mathbb{R}^{n(n-3)}$ represent the measured voltages at the boundary with n reprsents the number of electrodes considered in the system, the general output least squares approach can be written as

$$\sigma^* = \arg\min_\sigma \frac{1}{2}\|V_{\text{meas}} - F(\sigma)\|_2^2$$

The least-squares formulation fails to provide good reconstruction as the problem is severely ill-posed. Regularization is commonly performed to make the problem well-posed, and the objective function can be written as

$$\sigma^* = \arg\min_\sigma \frac{1}{2}\|V_{\text{meas}} - F(\sigma)\|_2^2 + \lambda G(\sigma)$$

where i) $G(\sigma) = \|\sigma - \sigma_0\|_2$ for quadratic regularization, where σ_0 is the reference conductivity ii) $G(\sigma) = \|\sigma - \sigma_0\|_1$ for L_1-norm regularization and iii) $G(\sigma) = \|\nabla\sigma\|_2$ for TV-norm regularization where $\nabla\sigma$ represents the gradient of the conductivity vector. Apart from these methods, L_1-norm constraint is also considered on the data-fit in (Borsic and Adler, 2012), which makes the reconstruction robust to outliers in the data. Unlike these methods wherein a convex relaxation of sparsity constraint is considered, the method described in (Varanasi et al., 2019) applies a sparsity constraint directly into the optimization problem.

2.2 Methodology

The main objective of EIT reconstruction is to estimate the conductivity vector given voltage-current measurements on the boundary. In the current paper, the idea of incorporating sparse constraint directly into the optimization is considered. A 1-norm constraint on the data-fit term is chosen to make the reconstruction more accurate in the presence of sharp changes in conductivity distribution and to make the algorithm robust to the outliers in the data.

The objective function is considered to be

$$\arg\min_\sigma \sum_{i=1}^{n} |V_{\text{meas},i} - F(\sigma)_i| \text{ subject to } \|\Delta\sigma\|_0 \leq s$$

where, n is the total number of measurements. Here, $\Delta\sigma$ $\Delta\sigma = \mathbf{A}\sigma$ where $\mathbf{A}$ is an upper bidiagonal matrix with -1 on main diagonal, $+1$ on the upper diagonal and zeros elsewhere. Therefore, the objective function is,

$$\arg\min_\sigma \sum_{i=1}^{n} |V_{\text{meas},i} - F(\sigma)_i| \text{ subject to } \|\mathbf{A}\sigma\|_0 \leq s$$

Denoting $\mathbf{A}\sigma = \hat{\sigma}$, the optimization problem can be reformulated as,

$$\arg\min_{\sigma,\hat{\sigma}} \sum_{i=1}^{n} |V_{\text{meas},i} - F(\sigma)_i| \text{ s. t. } \hat{\sigma} = \mathbf{A}\sigma \text{ and } \|\hat{\sigma}\|_0 \leq s$$

which can then be converted into the unconstrained form

$$\arg\min_{\sigma,\hat{\sigma},\|\hat{\sigma}\|_0\leq s} \sum_{i=1}^{n} |V_{\text{meas},i} - F(\sigma)_i| + \lambda\|\hat{\sigma} - \mathbf{A}\sigma\|_2^2$$

This problem involves joint minimization w.r.t σ and $\hat{\sigma}$ for a fixed λ. Hence a two step optimization is performed in which the objective function is minimized w.r.t σ in the first step and in the second step, the objective function is minimized w.r.t $\hat{\sigma}$ along with sparsity constraint.

Expressing mathematically, the optimization problem in step-1 (called as primal (P)) with fixed $\hat{\sigma}$ is

$$(P) \quad \arg\min_\sigma \sum_{i=1}^{n} |V_{\text{meas},i} - F(\sigma)_i| + \lambda\|\hat{\sigma} - \mathbf{A}\sigma\|_2^2$$

The expression can be modified for each i as,

$$|V_{\text{meas},i} - F(\sigma)_i| = \max_{x_i;\|x_i\|\leq 1} x_i\,(V_{\text{meas},i} - F(\sigma)_i)$$

Therefore, the objective function may be written as,

$$\min_{\sigma} \Big\{ \max_{x} \; x^T (V_{\text{meas}} - F(\sigma)) \\ + \lambda \|\hat{\sigma} - \mathbf{A}\sigma\|_2^2 \Big\}, \text{with } \|x_i\| \leq 1, i = 1, 2, \ldots, n \tag{1}$$

We now use the ideas of Primal-Dual Interior point technique presented in (Borsic and Adler, 2012). The details are given here for easy readability. Interchanging the min and max results into,

$$\max_{x} \Big\{ \min_{\sigma} \; x^T (V_{\text{meas}} - F(\sigma)) \\ + \lambda \|\hat{\sigma} - \mathbf{A}\sigma\|_2^2 \Big\}, \text{with } \|x_i\| \leq 1, i = 1, 2, \ldots, n \tag{2}$$

Computing the derivatives w.r.t primal variables and equating to zero results into,

$$J^T(\sigma)x + \lambda A^T(\hat{\sigma} - A\sigma) = 0$$

where $J(\sigma)$ is the Jacobian matrix of the forward model i.e., $F(\sigma)$. This results in the following equivalent optimization (called as dual problem (D))

$$(D) \quad \max_{x} \left\{ x^T (V_{\text{meas}} - F(\sigma)) + \lambda \|\hat{\sigma} - \mathbf{A}\sigma\|_2^2 \right\} \\ \text{with } \|x_i\| \leq 1, i = 1, 2, \ldots, n \\ J^T(\sigma)x + \lambda A^T(\hat{\sigma} - A\sigma) = 0$$

Instead of minimizing the primal or maximizing the dual, a complimentary condition obtained from the primal-dual gap is enforced in the optimization (Andersen et al., 2000).

$$G_{PD} = \sum_{i=1}^{n} |V_{\text{meas},i} - F(\sigma)_i| - x_i (V_{\text{meas},i} - F(\sigma)_i)$$

The *primal-dual* gap i.e., G_{PD} is zero if $V_{\text{meas},i} - F(\sigma)_i = 0 \; \forall i$ or

$$(V_{\text{meas},i} - F(\sigma)_i) - x_i \left(|V_{\text{meas},i} - F(\sigma)_i| \right) = 0 \\ \|x_i\| \leq 1, i = 1, 2, \ldots, n \\ J^T(\sigma)x + \lambda A^T(\hat{\sigma} - A\sigma) = 0 \tag{3}$$

The resulting equations in Eq. (3) are to be solved jointly on σ and x using for e.g. the Newton method. In order to estimate the derivatives, the absolute value in condition-1 of Eq. (3) needs to be smoothed. The smoothing is obtained by replacing the absolute value with $\sqrt{(V_{\text{meas}} - F(\sigma))^2 + \beta}$ with $\beta > 0$. The smoothed feasibility condition is known as *centering condition* which leads to a smooth pair of optimization problems (Andersen et al., 2000; Borsic and Adler, 2012). Therefore, the objective function is modified as

$$(V_{\text{meas},i} - F(\sigma)_i) - x_i \left(\sqrt{(V_{\text{meas}} - F(\sigma))^2 + \beta} \right) = 0 \tag{4}$$

$$\|x_i\| \leq 1, i = 1, 2, \ldots, n \tag{5}$$

$$J^T(\sigma)x + \lambda A^T(\hat{\sigma} - A\sigma) = 0 \tag{6}$$

Computing the partial derivatives w.r.t the variables, the final system of equations in the following form is obtained as,

$$\begin{bmatrix} -(I - XE^{-1}F)J(\sigma) & -E \\ -2\lambda A^T A & J^T(\sigma) \end{bmatrix} \begin{bmatrix} \delta\sigma \\ \delta x \end{bmatrix} \\ = - \begin{bmatrix} f - Ex \\ J^T(\sigma)x + \lambda A^T(\hat{\sigma} - A\sigma) \end{bmatrix} \tag{7}$$

with $X = \text{diag}(x_i)$, $f_i = V_{\text{meas},i} - F(\sigma)_i$, $F = \text{diag}(f_i)$, $E = \text{diag}\left(\sqrt{f_i^2 + \beta}\right)$. The above system of equations can be solved iteratively by computing the updates for $\delta\sigma$ and δx as

$$\delta\sigma = - \left[J^T E^{-1}(-I + XE^{-1}F)J - 2\lambda A^T A \right]^{-1} \\ \left[J^T E^{-1} f + 2\lambda A^T(\hat{\sigma} - A\sigma) \right] \\ \delta x = E^{-1} f - x - E^{-1}(I - XE^{-1}F)J\delta\sigma \tag{8}$$

A traditional line search procedure can be applied while updating the primal variable at k^{th} iteration as

$$\sigma^{(k+1)} = \sigma^{(k)} + \lambda_\sigma \delta\sigma^{(k)} \tag{9}$$

where λ_σ is the computed step length. The dual variable can be updated as

$$x^{(k+1)} = x^{(k)} + \min(1, \phi^*)\delta x^{(k)} \tag{10}$$

where ϕ^* is a scalar value such that

$$\phi^* = \sup \left\{ \phi : |x_i^{(k)} + \phi \delta x_i^{(k)}| \leq 1, i = 1, 2, \ldots, n \right\}$$

Once the conductivity vector i.e., σ is estimated using the aforementioned method, the estimation of $\hat{\sigma}$ for a fixed sigma is performed in step-2. Therefore, the optimization in step-2 is

$$\arg\min_{\hat{\sigma}} \sum_{i=1}^{n} |V_{\text{meas},i} - F(\sigma)_i| \\ + \lambda \|\hat{\sigma} - \mathbf{A}\sigma\|_2^2 \text{ subject to } \|\hat{\sigma}\|_0 \leq s$$

Since the first term is independent of $\hat{\sigma}$, this minimization is exactly equal to

$$\min_{\|\hat{\sigma}\|_0 \leq s} \|\hat{\sigma} - \mathbf{A}\sigma\|_2^2 \tag{11}$$

It is easy to see that the solution $\hat{\sigma}$ is the best s-sparse approximation of $\mathbf{A}\sigma$, i.e., the vector containing the s-maximum absolute entries of $\mathbf{A}\sigma$ at the same locations and zeros elsewhere.

The overall algorithm in the case when $n_m = 1$ is as follows. Firstly, an initial guess of conductivity vector (σ) and conductivity gradient vector ($\hat{\sigma}$) is provided in step-1 based on TV-norm regularization and conductivity vector (along with dual variable) is updated using the Newton method as explained in Eq. (9) (as well as Eq. (10)). The difference in the conductivity vector is estimated using the updated conductivity vector. These steps are repeated until the error between two iterations is in tolerance range. The overall steps are depicted in Algorithm 1.

Algorithm 1 Algorithm for a fixed value of regularization parameter (λ)

- **Inputs**: Experimental/simulated data ($\mathbf{V}_{\text{meas}}$), magnitude of current injected and the pattern of injection, termination criterion..
- **Output:** Conductivity vector.
- Initialize σ_0, $l = 0$ and define error$_2$ = $\|\hat{\sigma}_{l+1}^k - \hat{\sigma}_l^k\|_2^2$ and error$_1$ = $\|\sigma_l^{k+1} - \sigma_l^k\|_2^2$.

  while error$_2$ > tolerance, **do**
  - * Estimate $\hat{\sigma}_l^k$ by solving Eq. (11) with $\sigma = \sigma_l^k$

    while error$_1$ > tolerance, set $k = 0$ **do**
    - Compute σ_l^{k+1} and x_l^{k+1} using Eqs. (9) and (10)

    $k + 1 \longleftarrow k$

    end while

  $l + 1 \longleftarrow l$

  end while

  return conductivity vector σ

In the overall algorithm depicted in Algorithm 1, error$_1$ and error$_2$ are the errors between two consecutive iterations of σ_l^k and $\hat{\sigma}_l^k$ respectively.

2.3 Selection of Regularization parameter

Following the same approach for parameter estimation as in (Ramsay et al., 2007; Varanasi and Jampana, 2018), the regularization parameter (λ) is varied, starting from a low value to a very high value. For every λ, the optimization is performed, and the solution is considered as the initial guess for the next iteration. The iterations are repeated until a stopping criterion is met, i.e., the root mean square error (RMSE) value (defined in Eq. (12)) is in tolerance range, or the data fit error starts increasing after hitting a minimum value between two consecutive λ values.

3. CASE STUDIES

An EIT system with sixteen electrodes arranged on a plane with equidistant spaces and adjacent stimulation pattern, i.e., current is injected between adjacent pairs of electrodes and voltage is measured among all other successive pairs of electrodes is considered. The forward model (PDE) considered in this study was a finite element model with a circular pattern that is implemented in EIDORS software (Adler and Lionheart, 2006).

The proposed method is tested on two case studies, as shown in Fig. 1, and root mean square error (RMSE) is used to evaluate the performance.

$$\text{RMSE} = \sqrt{\frac{1}{n}\sum_{k=1}^{n}(V_{\text{data},k} - V_{\text{model},k})^2} \qquad (12)$$

Here, n denotes the length of the measurement vector. $V_{\text{data},k}$ and $V_{\text{model},k}$ represent the k^{th} element of the actual and estimated potential with the identified conductivity vector respectively. The value of λ (the regularization parameter) is steadily increased (in terms of order of 10 starting with 1×10^{-4}) and for every λ, the optimization as defined in Algorithm 1 is performed.

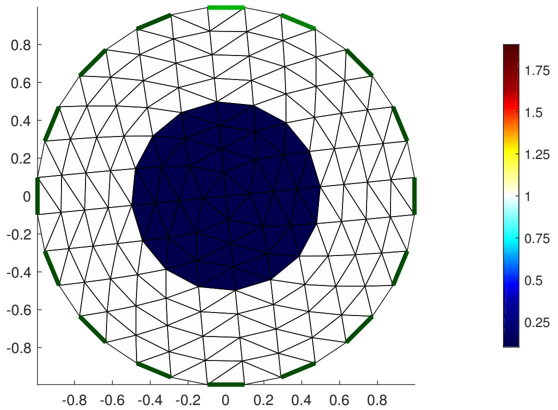

(a) *Case-1* : Air core in hydrocyclone

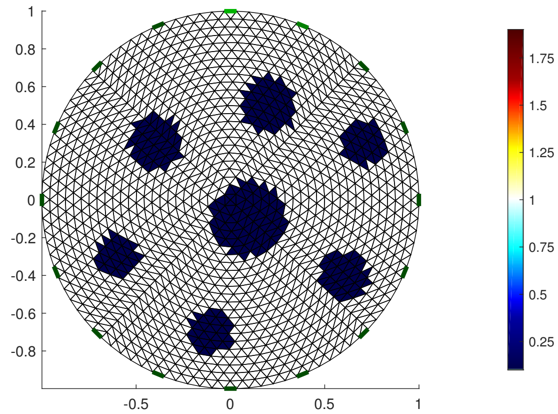

(b) *Case-2* : Bubbles in liquid

Fig. 1. Images of 2D phantoms for generating simulated data

The estimated conductivity vector is clustered into the number of objects considered to compute the absolute conductivity of the object. As each cluster signifies an object, the absolute conductivity of the object in a specified cluster is considered to be the average of conductivity values in that specified cluster.

3.1 Reconstruction results

Case-1: A phantom model of air-core in hydrocyclone, as shown in Fig. 1(a) is simulated to obtain the voltage data. The radius of the air core is modeled to be 0.5 m, and the conductivity of air is 0.1 S/m. The surrounding medium around the air core is water with a conductivity value of 1 S/m.

From the reconstructed image in Fig. 2, it can be concluded that the proposed method has provided sharp conductivity profiles by which we can have a reliable estimate of the air core size in an operating hydrocyclone. The air core size can be inferred from the radial conductivity profile of the hydrocyclone. The absolute conductivity of the object using the proposed method is 0.0718 S/m, and an RMSE value of 0.0034 is obtained.

Case-2: The other case study considered is bubbles in a circular pipe system, as shown in Fig. 1(b). The conductivity of the continuous medium and the dispersion phase (bubbles) are considered as 1 S/m and 0.1 S/m, respectively. The reconstructed image from the voltage

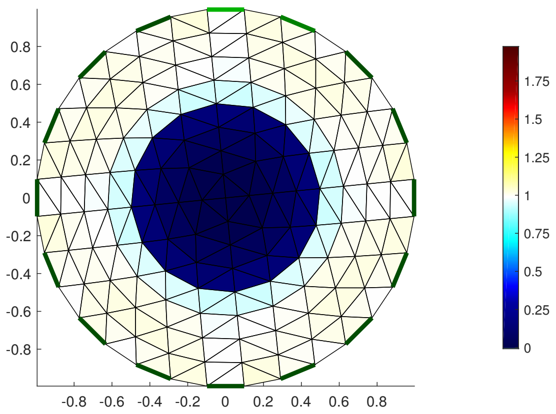

Fig. 2. Reconstructed image using the proposed method for *Case-1*

data is shown in the Fig. 3 and an estimated absolute conductivity of the bubble is obtained as 0.1818 S/m, and an RMSE value of 0.000819 is obtained.

It can be further noted from Fig. 3, the proposed algorithm has identified all the bubbles and also, the edge discontinuities of the bubbles can be observed clearly.

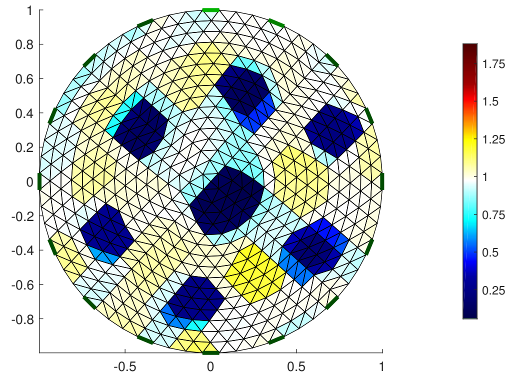

Fig. 3. Reconstructed image using the proposed method for *Case-2*

3.2 Reconstruction results with Outliers in data

To further demonstrate the accuracy of the proposed method in reconstruction with outliers in data, noise (Gaussian), is added to 10% of electrodes, and Monte-Carlo simulations are performed. The mean and the standard deviation of the RMSE values for *Case-2* is estimated to be 0.0444 and 0.0165, respectively, and the reconstructed image with the mean conductivity vector is reported in Fig. 4.

From Fig. 4, it can be concluded that the proposed method can detect the objects even with outliers in the data. However, the phase boundaries are not as sharp as in the zero noise case.

4. COMPARISON

In this section, a comparison of the proposed method with the $L_1 - L_1$ method as explained in (Borsic and Adler, 2012) is presented. The reconstructed images using $L_1 - L_1$ method for *Case* $-$ *1* and *Case* $-$ *2* are shown in Figs. 5 and 6 respectively.

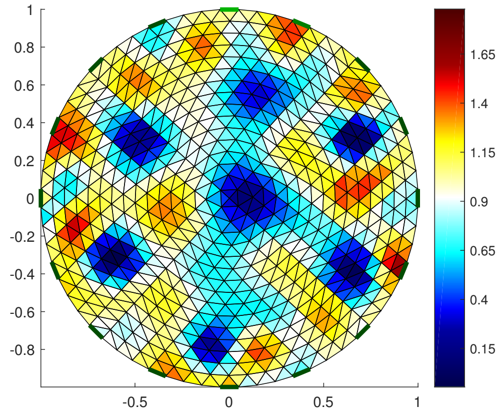

Fig. 4. Reconstructed image with mean conductivity using the proposed method for *Case-2* with outliers in data

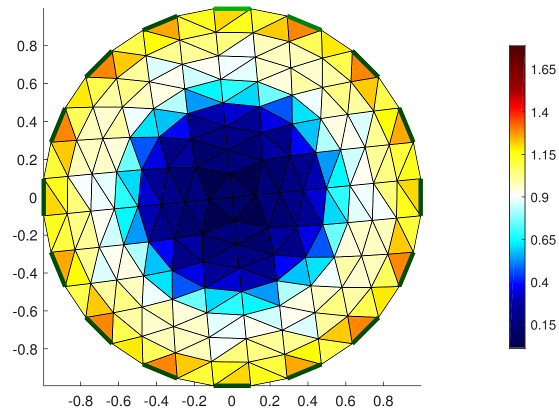

Fig. 5. Reconstructed image for *Case* $-$ *1* with $L_1 - L_1$ method

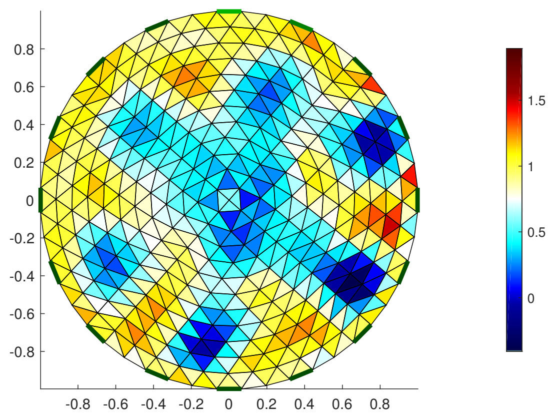

Fig. 6. Reconstructed image for *Case* $-$ *2* with $L_1 - L_1$ method

The absolute conductivities of objects is estimated to be 0.3009 S/m and 0.3977 S/m and RMSE values of 0.0151 and 0.2394 are obtained for *Case* $-$ *1* and *Case-2* respectively. From Figs. 2, 3, 5 and 6, it can be concluded that the proposed method is able to reconstruct the images with relatively high accuracy.

The L_2-sparse (Varanasi et al., 2019) method uses the 2-norm for the data fit term instead of the 1-norm in the objective function while including the sparsity constraint similar to the present method. A comparison was also made with this method. However, the results were very similar and, therefore, are not displayed again.

4.1 Outliers in data case study

A comparative study for *Case* $-$ *2* with outliers in the data with $L_1 - L_1$ and L_2-sparse methods is also performed. The mean and standard deviation of the RMSE values for *Case* $-$ *2* with $L_1 - L_1$ method is estimated to be 0.2806 and 0.0413 respectively whereas with the L_2-sparse method, these values were 0.0554 and 0.1494. The reconstructed image with the mean of the estimated conductivity with $L_1 - L_1$ and L_2-sparse are reported in Figs. 7 and 8 respectively.

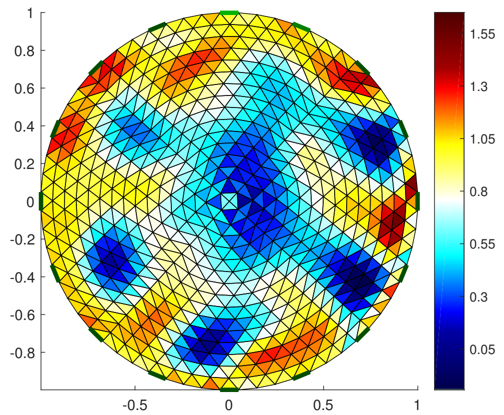

Fig. 7. Reconstructed image using $L_1 - L_1$ method with outliers in data

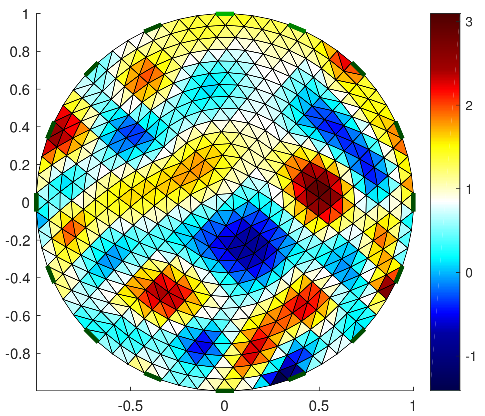

Fig. 8. Reconstructed image using L_2-sparse method with outliers in data

From Figs. 4, 7 and 8, it can be noted that the proposed method is able to detect the objects more accurately even in the presence of outliers in the data, and the RMSE values are also smaller compared to the existing methods.

5. CONCLUSIONS

In this paper, an L_1-sparse image reconstruction method for Electrical Impedance Tomography from the measured current-voltage data is described. The method considers an L_1- norm on the data fit term along with a direct sparsity constraint on the gradient of the conductivity distribution. Simulations on phantoms of air core in hydrocyclone and bubbles in liquid were reported, and it was observed that the proposed method results in more accurate conductivity profiles compared to an existing technique. The performance of the method is also tested when some of the measurements are corrupted by noise. Again, it was observed that the proposed method resulted in a better reconstruction of the conductivity distribution.

6. ACKNOWLEDGEMENTS

This research has been pursued with the support of the Department of Science and Technology (India) under the project *CRG/2018/004892*. We are incredibly thankful to DST for support.

REFERENCES

Adler, A. and Lionheart, W.R. (2006). Uses and abuses of eidors: an extensible software base for EIT. *Physiological measurement*, 27(5), S25.

Andersen, K.D., Christiansen, E., Conn, A.R., and Overton, M.L. (2000). An efficient primal-dual interior-point method for minimizing a sum of euclidean norms. *SIAM Journal on Scientific Computing*, 22(1), 243–262.

Bera, T.K. (2018). Applications of electrical impedance tomography (eit): A short review. In *IOP Conference Series: Materials Science and Engineering*, volume 331, 012004. IOP Publishing.

Borsic, A. and Adler, A. (2012). A primal–dual interior-point framework for using the l1 or l2 norm on the data and regularization terms of inverse problems. *Inverse Problems*, 28(9), 095011.

Borsic, A., Graham, B.M., Adler, A., and Lionheart, W.R. (2010). In vivo impedance imaging with total variation regularization. *IEEE transactions on medical imaging*, 29(1), 44–54.

Kotre, C. (1994). Eit image reconstruction using sensitivity weighted filtered backprojection. *Physiological measurement*, 15(2A), A125.

Ramsay, J.O., Hooker, G., Campbell, D., and Cao, J. (2007). Parameter estimation for differential equations: a generalized smoothing approach. *Journal of the Royal Statistical Society: Series B (Statistical Methodology)*, 69(5), 741–796.

Santosa, F. and Vogelius, M. (1990). A backprojection algorithm for electrical impedance imaging. *SIAM Journal on Applied Mathematics*, 50(1), 216–243.

Vadlakonda, B. and Mangadoddy, N. (2018). Hydrodynamic study of three-phase flow in column flotation using electrical resistance tomography coupled with pressure transducers. *Separation and Purification Technology*, 203, 274–288.

Varanasi, S.K. and Jampana, P. (2018). Identification of parsimonious continuous time LTI models with applications. *Journal of Process Control*, 69, 128–137.

Varanasi, S.K., Manchikatla, C., Polisetty, V.G., and Jampana, P. (2019). Sparse optimization for image reconstruction in electrical impedance tomography. *IFAC-PapersOnLine*, 52(1), 34–39.